DMD Fast Forward. Published on February 11, 2008 as doi:10.1124/dmd.108.020347

In vitro Metabolism of Licofelone (ML3000), an Inhibitor of Cyclooxygenases-1 and -2 and 5-Lipoxygenase

Wolfgang Albrecht, Anke Unger, Andreas K. Nuessler*, and Stefan Laufer

c-a-i-r biosciences GmbH, Paul-Ehrlich-Str. 15, 72076 Tuebingen, Germany (AU, WA), University of Tuebingen, Institute of Pharmacy, Auf der Morgenstelle 8, 72076 Tuebingen, Germany (SL), Department of General, Visceral and Transplantation Surgery, Charité, Campus Virchow Klinikum, Humboldt University Berlin, Berlin, Germany (AKN)* and Merckle GmbH, Department of Drug Research, 89079 Ulm, Germany (WA)

Running Title Page

Running Title:

Metabolism of licofelone in animal species and humans

Corresponding author:

Wolfgang Albrecht

c-a-i-r biosciences GmbH

Paul-Ehrlich-Str. 15

72076 Tübingen

Germany

Phone: +49 (-7071) 965 2081

Fax: +49 (-7071) 965 2089

e-mail: w.albrecht@cair-biosciences.de

Number of text pages: 28

Number of tables: 7

Number of figures: 5

Number of references: 36

Number of words

Abstract: 223

Introduction: 649

Discussion: 1131

List of nonstandard abbreviations used in the text:

ACN (acetonitrile), CIM (Cynomolgus monkey intestinal microsomes), CLM (Cynomolgus monkey liver microsomes), DLM (Beagle dog liver microsomes), ESI (electrospray ionization), HIM (human intestinal microsomes), HKM (human kidney microsomes), HLM (human liver microsomes), HLuM (human lung microsomes), ISTD (internal standard), MLM (CD-1 mouse liver microsomes), NZLM (New Zealand White rabbit liver microsomes), RLM (Sprague-Dawley rat liver microsomes), UDPGA (uridine-5'-phosphate glucuronic acid), UGT (UDP-glucuronosyltransferase)

Abstract

Licofelone (2-[6-(4-chlorophenyl)-2,2-dimethyl-7-phenyl-2,3-dihydro-1H-pyrrolizin-5-yl] acetic acid) is a dual inhibitor of both cyclooxygenase isoforms (COX-1/-2) and 5-lipoxygenase (5-LOX) and under development for treatment of osteoarthritis. In conventional *in vitro* assays using liver microsomes and NADPH as cosubstrate, a high metabolic stability of licofelone was observed. In the presence of UDP-glucuronic acid (UDPGA), licofelone is rapidly converted into the corresponding acyl glucuronide, M1. These results are in conflict with data from clinical studies. After administration of licofelone to humans, M1-plasma concentrations were negligibly low while the exposure of the hydroxy-metabolite M2 achieved values of approx. 20 % compared to that of the parent drug. Metabolism studies with human hepatocytes and dual-activity assays with microsomes, which allowed the simultaneous monitoring of hydroxylation and glucuronidation reactions, were performed and the metabolic pathway of licofelone was elucidated. After glucuronidation, predominantly catalyzed by UGT-isoforms 2B7, 1A9 and 1A3, M1 is converted into the hydroxy-glucuronide M3 in a CYP2C8 dependent reaction. The enzyme specificities were investigated using recombinant human CYP and UGT-isoforms as test systems. *In vitro* drug-interaction studies using the 6α-hydroxylation of paclitaxel as control reaction confirmed that neither licofelone nor M1 are relevant inhibitors of CYP2C8. The formation of M3 was also observed with liver microsomes from Cynomolgus monkeys but in incubations with mouse and rat liver microsomes, M1 remained unchanged. The clinical relevance of these findings is discussed.

Introduction

Licofelone (ML3000) is a dual inhibitor of cyclooxygenases (COX-1 and COX-2) and 5-lipoxygenase (5-LOX). Anti-inflammatory drugs with this mode of action are considered as attractive therapeutics for the treatment of arthritic diseases (Clària and López-Parra, 2005; Skelly and Hawkey, 2003). Almost three decades ago, the very first COX-/5-LOX-inhibitor benoxaprofen entered the market and, at that time, compared to the conventional non-steroidal anti-inflammatory drugs (NSAIDs), this compound not only showed equivalent efficacy but also an advantageous gastro-intestinal safety profile. Unfortunately, this compound was hepatotoxic which led to its withdrawal from the market (Bakke *et al*., 1995). In the late 80s, several companies were running drug-discovery programs to develop dual COX/LOX-inhibitors as NSAIDs with an improved gastro-intestinal safety. Most projects were terminated after the discovery of the inducible COX-2 and its identification as that isoform which is directly linked with the inflammatory process. After demonstrating advantageous gastro-intestinal safety in a series of clinical trials, COX-2-selective drugs (coxibs) achieved blockbuster-drug status very soon after entering the market. Today, it is known that all coxibs are burdened with a very low but unequivocal risk to induce life-threating or fatal cardiovascular events.

Apart from the first clinical experience with benoxaprofen, there is a lot of non-clinical and clinical evidence, that dual inhibition of the COX- and 5-LOX-pathway combine the advantages of conventional NSAIDs and coxibs, i.e. good anti-inflammatory, analgesic activity and gastro-intestinal as well as cardiovascular safety. As a promising candidate, licofelone (ML3000) has been developed for treatment of arthritic conditions. The mechanism of action of licofelone, i.e. inhibition of both COX-1/-2 and 5-LOX, was demonstrated in pharmacological studies as well as in experimental disease models (Tries *et al*., 2002; Kulkarni and Singh, 2007). Human and veterinary clinical trials confirmed the efficacy of

licofelone for treatment of osteoarthritis (Alvaro-Gracia, 2004; Moreau et al., 2007) as well as its advantageous gastro-intestinal tolerability (Bias *et al*., 2004; Moreau *et al*., 2005).

To date, no data regarding clinical and non-clinical pharmacokinetics and metabolism have been published. In humans, after oral administration of immediate release tablets, licofelone is rapidly absorbed from the gastro-intestinal tract and maximum plasma concentrations are achieved approx. 2-3 h after administration. Systemic elimination follows bi-phasic characteristics with a rapid initial decline of plasma concentration ($T_{½}(\alpha)$ = 1 h) and a slow terminal elimination ($T_{½}(\beta)$ = 7-9 h). In plasma, after single dosing, ML3000-1-O-acyl glucuronide (M1) and Hydroxy-ML3000 (M2) were detected as metabolites. Relative to the parent drug, the systemic exposure remained below 2%. After repeated administration, at steady-state, the exposure of M2 increased to approx. 20% relative to that of the parent drug and the rate of systemic elimination was below that of the parent drug (monophasic, $T_{½}$ = 10-12 h). In contrast, M1 remained at the level of a trace metabolite. In that respect the disposition of licofelone in humans is different from all standard animal species (mouse, rat, dog, monkey) in which systemic concentrations of M2 were negligible even upon chronic dosing. A further hydroxy metabolite of licofelone is M4. This compound was initially identified in microsomal experiments but not in plasma samples from humans after single and repeated administration of therapeutic doses, i.e. 200 mg or 400 mg b.i.d. Relevant concentrations were determined in plasma samples from subjects who were treated with increasing doses in order to determine the maximum tolerated dose. The chemical structures of licofelone and its metabolites are shown in figure 1. In the present article, results from *in vitro* metabolism studies are presented which demonstrate that in humans hydroxylation of the glucuronide M1 represents the pivotal step in the biosynthesis of M2. Although the cytochrome P-450 (CYP)-dependent hydroxylation of glucuronides has been described in the literature (Kumar *et al*., 2002, Delaforge *et al*., 2005), the formation of M2 represents a

unique example as the systemic exposure of humans to this major metabolite is based on the glucuronidation of the parent drug followed by hydroxylation of the glucuronide.

Materials and Methods

Chemicals and Enzyme Preparations

Licofelone (ML3000, 2-[6-(4-Chlorophenyl)-2,2-dimethyl-7-phenyl-2,3-dihydro-1H-pyrrolizin-5-yl] acetic acid) and the metabolites M1, M2 and M4 as well as ML3000 formic acid, diclofenac and 4'-hydroxy diclofenac were from Merckle (Ulm, Germany). Alamethicin, paclitaxel, β-NADPH, β-NADP, glucose-6-phosphate (G6P), glucose-6-phosphate dehydrogenase (G6P-DH), UDP-glucuronic acid (UDPGA) and recombinant human UDP-glucuronosyltransferases UGT1A1, UGT1A6, UGT1A7 and UGT1A10 were obtained from Sigma (Taufkirchen, Germany). Montelukast was extracted from SINGULAIR® 10 mg tablets. Recombinant human Cytochrome P450 Supersomes CYP1A2, CYP2A6, CYP2C8, CYP2C9*1, CYP2C19, CYP2D6*1, CYP3A4, CYP2J2, and CYP4F12, lymphoblast-expressed human CYP2B6 and CYP2E1, recombinant human UGT1A3, UGT1A9, UGT2B7 and UGT2B15 as well as pooled liver microsomes from male Beagle dogs (DLM) and male New Zealand white rabbits (NZLM) were purchased from BD Gentest (Heidelberg, Germany). Pooled human intestine (HIM), kidney (HKM) and lung (HLuM) (smokers) microsomes were purchased from In Vitro Technologies (Baltimore, USA). All other chemicals used were of the highest purity grade available.

Preparation of Liver Microsomes

Pooled liver microsomes from humans (HLM), Cynomolgus monkeys (CLM), Sprague-Dawley rats (RLM) and CD-1 mice (MLM) were prepared by differential centrifugation of homogenized liver samples according to previously described procedures (Pearce et al., 1996; Wilson et al., 2003). Cynomolgus monkey intestine microsomes (CIM) were prepared from monkey mucosa homogenate. Protein content was determined according to the Bradford assay (Bradford, 1976) with bovine serum albumin as standard.

Biotransformation in human hepatocytes

Primary human hepatocytes were isolated from liver samples obtained from patients undergoing partial liver resections according to a two-step collagenase perfusion technique and cultivated in 6-well plates (1 x 106 cells per well), After the attachment period, the culture medium was changed and 30 µM and 100 µM licofelone dissolved in methanol were added (final solvent concentration 0.5 %). Plates were incubated at 37 °C (5 % CO_2 in air, 95 % relative humidity) and samples (100 µl) were withdrawn after 1 h and 4 h. For final sampling, reactions were terminated after 24 h by addition of 0.5 vol of ice cold methanol. The cells were carefully scraped off the plates and the suspensions were transferred into reaction tubes. Each experiment was performed in triplicate with cells isolated from liver samples of three different donors. After addition of ML3000 formic acid as internal standard (ISTD), protein was precipitated with acetonitrile (ACN). Samples were centrifuged and the supernatant was analyzed by LC-MS/MS.

Phase I in vitro Metabolism Experiments and Dual Activity Assays

Phase I metabolism experiments and dual activity assays were carried out in 0.1 M Tris-HCl buffer (pH 7.4, 37 °C) containing 0.1 % BSA, 25 µg/ml alamethicin, 4 mM $MgCl_2$, 5 mM UDPGA and 1 mM β-NADPH at a final volume of 250 µl. For phase I metabolism assays no UDPGA was added. All incubations were performed with HLM, CLM, RLM, MLM, DLM, NZLM, HIM, HKM, HLuM as well as CIM. Final microsomal protein concentration was 1 mg/ml each. For activation of microsomal UDP-glucuronosyltransferases (UGTs), samples were pre-incubated on ice for 15 min. After pre-warming to 37 °C, reactions were started by addition of licofelone dissolved in methanol (final solvent concentration 1 %). Final concentrations were 10 µM, 30 µM, and 100 µM. After 30 min, an aliquot was withdrawn and

mixed with ISTD and 1.0 vol of cold ACN. Precipitated protein was removed by centrifugation and the supernatant was analyzed with LC-MS/MS. All experiments were performed in triplicate. In a preliminary experiment no influence on phase I metabolism reactions in case of pre-incubation on ice in the presence of alamethicin could be observed (data not shown).

Metabolism Experiments with M1

HLM, CLM, RLM and MLM (1 mg/ml each) were incubated with 3 µM M1 in 0.1 M Tris-HCl buffer (pH 7.4, 37 °C) containing 0.1 % BSA, 1 mM β-NADPH, and 1 mM $MgCl_2$ at a final volume of 250 µl. Reactions were initiated by addition of substrate dissolved in methanol (final solvent concentration 1 %). Each experiment was performed in duplicate. Sample preparation was performed as described above. In a control experiment, M1 was incubated in 0.1 M Tris-HCl buffer only.

Phase I-assays with licofelone and recombinant cytochrome P450 (CYP) isoforms

Incubations with CYP1A2, CYP1A6, CYP2B6 (62.5 pmol/ml each), CYP2C8, CYP2C9*1, CYP2C19, CYP2D6*1, CYP2E1 (127.5 pmol/ml each), CYP2J2, CYP4F12 and CYP3A4 (50 pmol/ml each) were carried out in 0.1 M Tris-HCl buffer (pH 7.4, 37 °C) containing 1 mM $MgCl_2$,1 mM β-NADPH and 0.1 % BSA. Reactions were started by addition of 10 µM licofelone dissolved in methanol (final solvent concentration 1 %) at a final concentration of 3 µM and 10 µM. After 30 min, reactions were terminated as described above. Additional assays with CYP2C8, CYP2C9*1, CYP2C19, CYP2D6*1, CYP2J2, and CYP3A4 were performed with 100 µM licofelone in the presence of 50 pmol/ml P450 as well as 200 pmol/ml P450. Samples preparation was performed as described above.

Phase II-assays with licofelone and recombinant UGT-isoforms

Experiments with UGT1A1, UGT1A3, UGT1A6, UGT1A7, UGT1A9, UGT1A10, UGT2B7 and UGT2B15 were carried out in 0.1 M Tris-HCl buffer pH 7.4 in the presence of 4 mM $MgCl_2$, 5 mM UDPGA and 25 µg/ml alamethicin at a. final protein concentration of 1.0 mg/ml each. UGTs were activated by incubation on ice in the presence of alamethicin and $MgCl_2$ for 15 min. After addition of UDPGA, samples were pre-warmed to 37 °C and reactions were initiated by addition of 100 µM licofelone dissolved in methanol (final solvent concentration 1 %). Samples were incubated for 30 min and processed as described above.

Inhibition Experiments

Montelukast: A dual activity assay was performed with 30 µM licofelone as described above. Immediately prior to the addition of the substrate, montelukast was added to the incubation mixtures. Final concentrations were 0, 1, 10, and 30 µM a final methanol concentration of 1.5 %. After incubation for 30 min, samples were analyzed by LC-MS/MS.

M1: 10 µM and 30 µM M1 were incubated with HLM (1 mg/ml) and CYP2C8 (50 pmol/ml) as described above. In a modified experiment, M1 was pre-incubated at 37 °C in the presence of HLM and CYP2C8, respectively. After 15 min, reactions were started by addition of β-NADPH and samples were incubated for 30 min.

Paclitaxel-Assay: The paclitaxel-6α-hydroxylation was investigated in HLM and with CYP2C8. Standard assays were performed in 0.1 M Tris-HCl buffer pH 7.4 with addition of 0.1 % BSA and in the presence of 4 mM $MgCl_2$. A NADPH-regenerating system was established by addition of 5 mM G6P, 1 mM NADP and 1 U/ml G6P-DH. Final substrate concentration was 50 µM in a final volume of 250 µl. After 30 min, reactions were terminated by addition of 125 µl of cold ACN. Samples were vortexed, centrifuged and the supernatant was subjected to HPLC/UV analysis.

Metabolite production for paclitaxel was linear with respect to time, microsomal protein and cytochrome P450 concentration. The assay was validated using montelukast as CYP2C8 inhibitor (data no shown) With 100 µM montelukast, a remaining enzyme activity of 15 % was determined. Interaction experiments were performed with 10, 30, and 100 µM licofelone (dissolved in methanol) in comparison with a control assay with addition of solvent only. All assays were performed in triplicate and mean values and standard deviations were calculated.

LC-MS/MS Analysis

Chromatographic separation of licofelone metabolites was achieved on an Inertsil ODS-2 column (60 x 4.6 mm, dp = 5 µm) with a WiCom OptiGuard C18, 1 mm guard column using an Agilent 1100 high performance liquid chromatography system. Mobile phase A consisted of ACN containing 1 % formic acid, mobile phase B consisted of deionized water adjusted to pH 4.0 with formic acid. The gradient profile was %B (t[min]) 60(0)-60(1)-40(2)-40(7)-25(8)-25(10)-10(11)-10(14)-60(14.1)-60(20) at a flow rate of 0.4 ml/min. Analytes were detected using a Thermo LCQDuo ion trap mass spectrometer with electrospray ionization (ESI) in positive ion mode. ESI conditions were set as follows: spray voltage of 4.5 kV, sheath gas flow 90 units, auxiliary gas flow rates 20 units, capillary temperature 280 °C with a voltage of 20 V. Column effluent was split 1:3 between mass spectrometer and waste. The mass transitions used were m/z 380.3 → 334.1 for licofelone, 556.1 → 380.0 for M1, 396.1 → 350.1 for M2 and M4, 572.1 → 396.0 for M3 and M5 as well as 366.3 → 348.2 for the ISTD. Collision energy was set to 35 % each. Rates of M2 and M4 formation were quantified by comparison of peak area ratios of the incubation samples to those of known concentrations of reference compounds. Calibration samples were processed in the same way as described for incubation samples. Calibration curves were linear over the concentration range used (r^2 > 0.99). Due to the lack of adequate reference compounds for quantitation of M1 and M3, a

mean glucuronide conversion coefficient was established by comparison of free and total M2 concentration in selected microsomal incubation samples and samples from hepatocyte cultures, i.e. M2 concentrations were determined before after hydrolysis with 5 % NaOH (incubation at 50°C for 90 min). This coefficient was also applied to estimate M1 concentrations. In samples incubated with UGT isoforms only peak area ratios of M1 were determined.

HPLC/UV Analysis

Paclitaxel and 6α-hydroxy-paclitaxel were separated on a Phenomenex Synergi 4U MAX-RP 150 x 4.6 mm column with a mixture of methanol (A) and 0.01 M KH_2PO_4 buffer pH 2.3 (B) with a flow rate of 1.5 ml/min at 40 °C using a HP1090 instrument. The gradient profile was %B (t[min]) 35(0)-35(10)-10(14)-10(17)-35(19)-35(25), and the column effluent was monitored at 230 nm. Retention times of paclitaxel and metabolites were as follows: 3.60 min (3α-hydroxy-paclitaxel), 5.70 min (6α-hydroxy-paclitaxel) and 7.30 min (paclitaxel).

6α-hydroxy-paclitaxel concentrations were determined by means of external calibration using a calibration curve which was established by linear regression of concentration/peak area data pairs of paclitaxel reference standards. Similar extinction coefficients for paclitaxel and its hydroxy metabolites was concluded based on the fact that the sum of peak areas determined for paclitaxel and its metabolites 6α-hydroxypaclitaxel and 3-hydroxypaclitaxel remained essentially unchanged during microsomal metabolism assays.

Results

Phase I and phase II assays

Initial *in vitro* phase I-biotransformations using liver microsomes from rat and human demonstrated a high metabolic stability of licofelone. Two hydroxy metabolites, M2 and M4 were detected but concentrations, determined after 30 min or 60 min incubation of 0.1 - 100 µM licofelone reflected that less than 2 % of the substrate were converted. Assays with diclofenac were performed as control reactions (table 1). In incubations with HLM, only 0.06 % of the initial substrate concentrations were converted into M2 compared to 1.8 % M4. With RLM as test system, 1.1 % M2 and 1.8 % M4 were found. The formation of M4 was somewhat surprising because in plasma samples from laboratory animals, this metabolite was not detected and in humans, quantifiable concentrations were determined only in plasma samples which were collected during a clinical study after administration of supra therapeutic doses to determine the maximum tolerated dose.

To identify the metabolizing enzymes involved in the formation of hydroxy metabolites, experiments with different CYP-isoforms were performed. Although the direct hydroxylation of licofelone has been considered as a quantitatively negligible pathway, a primary screening experiment, conducted with 10 µM licofelone, gave evidence that CYP2C8, CYP2C9, CYP2C19, CYP2D6, CYP2J2 and CYP3A4 are involved in the oxidation of licofelone. Thus, in a second experiment, 100 µM licofelone were incubated in the presence of 200 pmol/ml of these isoenzymes. In all incubations, both hydroxy metabolites were detected but M4 concentrations always exceeded those of M2 (figure 2). With more than 600 ng/ml M4, which corresponds to a substrate turnover of approx. 1.6 %, CYP2C9*1 showed the highest activity towards formation of M4 followed by CYP2J2 > CYP3A4 > CYP2C8 > CYP2C19 > CYP2D6*1. However, M4 concentrations formed with CYP2J2, CYP3A4, CYP2C8,

CYP2C19 and CYP2D6*1 were less than the third compared to the amount found in incubations with CYP2C9*1. With 67.8 ng/ml, only CYP2J2 formed significant amounts of M2. CYP2C9*1 and CYP2C8 also formed M2, but to a much lower extent.

In vitro glucuronidations using microsomes demonstrated a rapid conversion of licofelone into the corresponding 1-O-acyl glucuronide, M1 (table 1). The chemical structure of this metabolite was previously demonstrated by analysis of biological samples and chemical synthesis (Kirschning *et al.*, 1997). Again, glucuronidation of diclofenac was used as a positive control (table 1). To identify the UGT isoforms involved in the formation of M1, 100 µM licofelone was incubated with different human recombinant UGT-isoforms. M1 concentrations were expressed as M1/ISTD peak area ratios and results are summarized in table 2. UGT isoforms 2B7, 1A9 and 1A3 were the most important enzymes. Minor activities were also observed with UGT 1A7 and 2B15. The determination of kinetic constants was not the objective of this UGT-screening assay.

Although the enzymes involved in the direct hydroxylation and glucuronidation of licofelone were identified, these data also demonstrated that standard assays with microsomes were not appropriate to explain the high exposure of M2 in humans. Therefore, experiments with freshly isolated human hepatocytes were performed.

Biotransformation of licofelone in human hepatocytes

Licofelone (3, 10 and 30 µM) was added to primary human hepatocytes and aliquots of the supernatant were analyzed by LC-MS. The rate of metabolite formation was not linear throughout the observation period but significantly declined after 4 h. Biotransformation rates which were derived from metabolite concentrations determined at 4 h and 24 h after

incubation of 30 µM and 100 µM licofelone, are given in table 3. The glucuronide M1 accounted for 85 % of the sum of metabolites and was clearly dominating after 24 hours. Both hydroxy metabolites M2 and M4 were present but, in contrast to phase I-metabolism experiments using microsomes, M2 concentrations substantially exceeded those of M4, in particular if corresponding glucuronides were considered. The observation that M3 concentrations substantially exceeded those of M2 was interpreted as a result of the high glucuronidation activity of hepatocytes. M5 was detected but throughout the observation period, concentrations remained below the limit of quantification.

The metabolite profile in experiments performed with 100 µM licofelone was almost identical, however, the total biotransformation was only about half of the rate observed with 30 µM. In addition, oxidative metabolism was less pronounced since M1 accounted for even more than 95 % of the overall metabolism.

Dual activity assays using liver microsomes

The metabolism experiments using human hepatocytes demonstrated that both biotransformation activities, *i.e.* hydroxylation and glucuronidation were required to achieve a M2/ M4 ratio which at least qualitatively reflects the human *in vivo* metabolism. However, the integrated phase I/II-metabolic capacity of hepatocytes does not allow the elucidation of metabolic pathways. Furthermore this test system is less suitable to identify the enzymes responsible for biotransformations of interest. Finally, hepatocytes from dogs, mice or monkeys are not ubiquitously available which limits their use for inter-species comparison of drug metabolism. Glucuronidation of xenobiotics is catalyzed by UDP-glucuronosyltransferases (UGTs), a superfamily of membrane-bound enzymes. UGTs largely reside at the luminal face of the endoplasmatic reticulum and both, the substrate and the co-

factor UDP-glucuronic acid (UDPGA) have limited access to the active centre. *In vitro*, high glucuronidation activities are generally achieved by addition of membrane-disrupting polyoxyethylene-based detergents like Brij or Triton X. However, this procedure has a substantial impact on CYP-activity and the simultaneous investigation of CYP- and UGT-catalyzed reactions was not possible. Substitution of these conventional ingredients with the channel-forming antibiotic alamethicin results in an activation of UGTs without affecting CYP-dependent biotransformations (Fisher *et al*., 2000). Thus, this dual-activity assay system was established and applied to investigate the metabolism of licofelone.

The experiments were performed with HLM, CLM, DLM, NZLM, RLM and MLM. As cofactors, NADPH and UDPGA were added. To determine the effect of the glucuronidation activity of each microsomal preparation, control experiments without UDPGA were included. The results obtained after incubation of 10 µM licofelone for 30 min are summarized in table 4. In the absence of UDPGA, no glucuronides were detected, and the extent of hydroxylation of licofelone was as low as observed in initial phase I assays. M2 was detected in liver microsomes from all species except for DLM, but in HLM and MLM, concentrations were below the limit of quantification. The most relevant biotransformation was observed in NZLM with a relative content of 8 % M2 and 0.18 % M4. Supplementation of UDPGA resulted in a completely different metabolite pattern. In HLM the overall biotransformation increased from 2.0 % to 34.9 % and the main metabolite was M3, *i.e.* the glucuronide of M2 (rel. content: 26.8 %). The content of M1 was 7.3 %. With microsomes from animal species, M1 was dominating the other metabolites. M3 was either not detected (DLM, RLM, MLM) or at comparably low concentrations (CLM, NZLM). This experiment strongly indicated principal differences between humans and animal species. Considering the M1 concentration, an ultra rapid glucuronidation of M2 appeared unlikely. Therefore, the only plausible explanation of this result was that M1 was hydroxylated to M3 followed by partial hydrolysis

of the acyl glucuronide which led to the determined concentrations of M2. In contrast to the experiments with HLM, with microsomes from monkey, rabbit and rat, M2 concentrations were lower in the presence of UDPGA, thus suggesting the opposite metabolic pathway, *i.e.* hydroxylation followed by glucuronidation.

With HLM, the experiment was repeated with licofelone concentrations of 30 and 100 µM. In figure 3, the biotransformation rates, relative to the initial substrate concentrations as well as the concentrations are given. With 10 and 30 µM licofelone, the sum of glucuronides (M1 + M3) was 3.41 µM and 9.92 µM, which correspond to biotransformation rates of 34% and 33%. With 100 µl licofelone, the relative glucuronide content was 25 %. The biotransformation rate of M2 and M3 decreased with ascending substrate concentrations. The highest M3-concentration (5.02 ± 0.11 µM) was observed at 30 µM while only 2.41 ± 0.56 µM were determined after incubation of 100 µM licofelone. These data indicate that the glucuronidation capacity of the test system was limited at concentrations above 30 µM. In contrast, hydroxylation of M1 was partly inhibited in incubations with 100 µM. M4-concentrations increased with ascending substrate concentrations in an almost proportional manner. The biotransformation rate to M4 was essentially constant.

In vitro Metabolism of M1

To confirm the proposed metabolic pathway, conventional phase I metabolism experiments with HLM, CLM, RLM and MLM at a concentration of 10 µM M1 were performed. M1 was prepared by enzymatic glucuronidation and purified by preparative HPLC. As summarized in table 5, a quantifiable extent of M1 hydroxylation into M3 was obtained with HLM (> 90 %) and CLM (35 %). In contrast, in incubations with MLM and RLM, only traces of M3 were detected. In control incubations in Tris-HCl buffer, M1 remained stable and did not show significant hydrolysis and a chemical oxidation was not observed at all. M5, the glucuronide

of M4, was not detected in any experiment. In addition, *in vitro* assays were performed with several CYP-isoforms, but the formation of M3 was only observed in incubations with CYP2C8 (50 %).

Inhibition of CYP2C8

Montelukast, a selective and potent CYP2C8 inhibitor (Walsky *et al.*, 2005a) was used to verify the observed CYP2C8-specificity of M1 hydroxylation. Dual activity assays with human liver microsomes were repeated without and with increasing montelukast concentrations. The effect of 1, 10 and 30 µM montelukast on the formation of M3 is shown in table 6. For M2 and M3, a concentration-dependent inhibition was obtained. In contrast, M1 concentrations increased with ascending inhibitor concentrations which reflects that only the hydroxylation of M1 rather than its UGT-mediated formation is affected by montelukast. To achieve a substantial effect on M2 and M3, at least 10 µM montelukast had to be added to the incubation mixture which is substantially above the reported Ki-value of 20 nM (Walsky *et al.*, 2005a). However, the inhibition potency of montelukast is strongly dependent on the protein concentration (Walsky *et al.*, 2005b). Using amodiaquine N-deethylation as model reaction, the IC_{50} increased from 0.23 µM at a protein concentration of 0.025 mg/ml to 18 µM at 2 mg/ml. In the dual-activity assays, the protein concentration was also 2 mg/ml (1 mg/ml microsomal protein in buffer containing 0.1 % BSA) and the observed 75% inhibition of M2 formation (0.11% instead of 0.45 %) and the 69 %-inhibition of M3 formation (8.1 % instead of 25.8 %) in the presence of 10 µM montelukast are in line with the published inhibition potency. In the presence of 30 µM montelukast M2 concentrations were below the limit of quantification.

The formation of M4 was also inhibited in a concentration-dependent manner by montelukast which can be explained by the involvement of CYP2C8 in this reaction but also by the inhibition of CYP2C9 at high montelukast concentrations (Walsky *et al.*, 2005a).

Influence of M1 on CYP2C8

In dual activity assays using HLM as well as in human hepatocytes, ascending substrate concentration led to a shift of relative concentrations of metabolites. At high licofelone concentrations, the relative content of M1 was higher compared to incubations at lower substrate concentrations. Accordingly, the relative concentrations of hydroxy metabolites decreased with ascending substrate concentrations. M1 is a 1-O-Acyl glucuronide and these metabolites are generally known to be chemically unstable. Dependent on the nature of the aglycon, a shift to C2, C3 and C4 of the glucuronic acid may occur and, as a final reaction, a transesterification of the aglycon to proteins, was described (Spahn-Langguth *et al.*, 1996; Bailey and Dickinson, 2003; Stachulski 2007). As shown above, as far as quantifiable with the applied analytical method, M1 remained stable during in vitro metabolism assays. To confirm this observation in a functional setting, 10 µM and 30 µM M1 were pre-incubated with human liver microsomes and recombinant CYP2C8 microsomes for 15 min prior to the addition of NADPH which triggers the hydroxylation activity. As shown in figure 4, in incubation with microsomes, M3 concentrations increased proportionally with the initial substrate concentration and pre-incubation had no impact on the reaction. In the analogous experiment with CYP2C8, M3 concentrations were similar at 10 and 30 µM but again, pre-incubation had no effect on the hydroxylation activity.

Effect of licofelone and M1 on paclitaxel-6α-hydroxylation

To evaluate the drug interaction potential of licofelone and M1 on CYP2C8-dependent reactions, the effect of both compounds on the 6α-hydroxylation of paclitaxel was investigated using the CYP2C8 standard probe substrate paclitaxel (Dai *et al.*, 2001). The results are illustrated in figure 5. In HLM and CYP2C8, licofelone inhibited the formation of 6α-hydroxypaclitaxel in a concentration dependent manner. In the presence of 10 µM licofelone, only a weak inhibition was observed and a licofelone concentration of 100 µM was required to achieve a substantial inhibition (approx. 80%) when compared to the control experiment. The effect of M1 on CYP2C8 activity was even less pronounced. A relevant inhibition was only observed at 100 µM. Control reactions with the CYP2C8-specific inhibitor montelukast verified the validity of this inhibition experiment. Systemic concentrations of licofelone- and M1 at or above 30 µM are not achieved in humans *in vivo* and therefore, a clinically relevant inhibition of CYP2C8 during therapeutic use of licofelone can be excluded.

Extra-hepatic Metabolism of licofelone

Results of dual activity assays performed with pooled microsomes from tissue samples of human intestine, kidney and lung as well as Cynomolgus monkey intestine are summarized in table 7. M1 was the major extra-hepatic metabolite. Both hydroxy metabolites of licofelone could not be detected in any of these incubation mixtures. With 33.0 % the highest extra-hepatic biotransformation was observed in HKM followed by HIM (21 %). While in HKM also traces of M3 could be detected, in HIM only M1 could be detected. HLuM did not show significant metabolism activity towards licofelone. Microsomes from monkey intestinal mucosa also showed substantial glucuronidation of licofelone. Low amounts of M3 were also determined. The total biotransformation in CIM was almost twofold higher compared to HIM.

With increasing licofelone concentrations, biotransformation rates in microsomes from extra-hepatic tissue also decreased as observed with liver microsomes.

Discussion

The results of *in vitro* metabolism experiments with licofelone demonstrated that glucuronidation of the carboxylic acid followed by CYP2C8-catalyzed hydroxylation of the acyl glucuronide M1 represents the primary elimination pathway of this compound. Direct hydroxylation to M2 and M4 was also observed in these metabolism experiments but, at least in humans, the contribution of these pathways to systemic clearance is negligible. A screening with recombinant CYP-isoforms provided qualitative information regarding licofelone hydroxylation enzymes but determination of the enzyme kinetic constants was not possible. At a substrate concentration of 100 µM (= 38,000 ng/ml), maximum metabolite concentrations of 600 ng/ml were observed with CYP2C9, which correspond to a relative conversion of 1.6%. At an initial concentration of 10 µM, only traces of hydroxylated metabolites were detected and the determination of valid conversion rates at a concentration range which would allow the determination of V_{max} and K_M was not possible. Therefore, the analysis was limited to the identification of all those CYP-isoforms which catalyze the formation of M2 and M4. Aryl hydroxylation of licofelone to M4, which was predominant in microsomal phase I assays was catalyzed, in decreasing order of importance by CYP2C9 >> 2J2 > 3A4 > 2C8 > 2C19 > 2D6. M4 was also found in incubations with liver microsomes from animal species. In plasma samples this metabolite was not detected. *In vivo*, a high glucuronidation-biliary excretion capacity may prevent a systemic exposure of this metabolite. M2 was detected, again in decreasing order, in incubations with CYP2J2 > 2C9 > 2C8. CYP2C-isoforms and CYP3A4 belong to the most important drug metabolizing enzymes but CYP2J2 is mainly known for its role in the metabolism of arachidonic acid into epoxyeicosatrienoic acid derivatives. The antihistamines astemizole and ebastine have been described as the first and only xenobiotic compounds that are metabolized by CYP2J2 (Matsumoto *et al.*, 2002; Hashizume *et al.*, 2002). The metabolism of licofelone by CYP2J2

also supports the hypothesis that the mechanism of dual inhibition of COX and 5-LOX is based on conformation similarities between licofelone and arachidonic acid (Laufer *et al.*, 1994).

In further functional assays using HLM and CYP-specific substrates (midazolam and testosterone for CYP3A4, diclofenac for CYP2C9, (S)-mephenytoin for CYP2C19 and dextromethorphan for CYP2D6), it was demonstrated that, up to concentrations of 30 µM, licofelone had no significant impact on the activity of these CYP-specific biotransformations (unpublished results). The effect of licofelone on the activity of CYP2J2 still remains to be investigated.

In vivo, the formation of M2 via the acyl glucuronide M1 represents the main pathway. The UGTs 2B7, 1A9 and 1A3 were identified as the most relevant isoforms involved in the formation of M1, an observation, which is in line with results of UGT-screenings with other carboxylic acids. Recently Kuehl *et al.* identified the UGT-isoforms involved in the acyl glucuronidation of eight different NSAIDs (Kuehl *et al.*, 2005). Apart from individual differences between the substrates, the isoforms UGT2B7, UGT1A3, UGT1A9 and UGT1A8 used all tested compounds as substrates. The rank order UGT2B7 >> UGT1A3 ≈ UGT1A9 for glucuronidation of carboxylic acids was also reported by Sakaguchi *et al.* (Sakaguchi *et al.*, 2004). UGT1A8 was not included in the present investigation but due to its low substrate specificity it may also be involved in the formation of M1.

Hepatically formed acyl glucuronides are generally excreted by carrier-mediated processes across either the canalicular or basolateral membrane (Zamek-Gliszczynski *et al.*, 2006) and it is hypothesized that this route is also dominating in the disposition of licofelone - both in

humans and animal species. *In vitro*-metabolism assays demonstrated that in humans, M1 is also hydroxylated to M3 in a CYP2C8-dependent reaction. This enzymatic step represents the pivotal step for the systemic availability of M2. The site of hydrolysis of M3 is not unequivocally clear. However, in biotransformations of licofelone with hepatocytes, M3 was the predominant metabolite which suggest that hepatocytes contain a low enzymatic activity towards M3-hydrolysis. Furthermore, in circulating blood of humans, only traces of M3 were found (unpublished data) which excludes the possibility that M3 enters the systemic circulation and is hydrolyzed by plasma esterases. Therefore, the biliary excretion of M3 and its hydrolysis in the intestinal tract followed by absorption of M2 remains the most likely pathway. This hypothesis is supported by the observation that after single administration of licofelone M2 plasma concentrations were low but became relevant after repeated, twice-daily drug administration.

Hydroxylation of either licofelone to M2 or M1 to M3 introduces a chiral centre (quaternary carbon in the pyrrolizine ring) into the molecule. The stereospecificity of this biotransformation, however, was not addressed in this study.

CYP2C8, which was identified as the only CYP isoform involved in M1 hydroxylation, was previously reported as the enzyme responsible for hydroxylation of diclofenac acyl glucuronide (Kumar *et al.*, 2005) and estradiol-17β-glucuronide (Delaforge *et al.*, 2005). Despite the similarity of the elimination pathway of diclofenac and licofelone, the results published by Kumar *et al.* demonstrate an important difference between these two drugs. In incubations with microsomes, a rapid degradation of diclofenac acyl glucuronide was observed, irrespective of the presence or absence of NADPH. This result can be most likely attributed to the known chemical instability of the acyl glucuronide (Grillo *et al.*, 2003). In

contrast, M1 remained stable throughout the incubation period of 60 min with dog and rat liver microsomes with or without supplemented NADPH.

Incubation experiments with different CYP isoforms as well as with liver microsomes in the presence of the CYP2C8 specific inhibitor montelukast demonstrated that hydroxylation of M1 is solely catalyzed by this isoform. In the liver, CYP2C8 constitutes approx. 7 % of the total microsomal CYP-content but its expression was also demonstrated in kidney, intestine, adrenal gland, brain, mammary gland, ovary, heart as well as in breast cancer tumors (Totah and Rettie, 2005). In dual activity assays with licofelone and HKM, M3 was identified as a metabolite which is in line with the reported CYP2C8 expression in kidneys. In contrast, with HIM, another potential CYP2C8 source, only the formation of M1 was observed.

CYP2C8 is involved in the metabolism of many drugs (Totah and Rettie, 2005) and therefore, CYP2C8 substrates should be investigated for their potential to cause clinically relevant drug interactions. For example, based on *in vitro* inhibition studies, it has been suggested that CYP2C8 inhibition by gemfibrozil acyl glucuronide substantially contributed to the severe toxicity of the lipid-lowering drug cerivastatin when co-administered with gemfibrozil (Ogilvie *et al.*, 2006; Shitara *et al.*, 2004). Based on the results of the present study, neither licofelone nor M1 modulate the activity of CYP2C8 at clinically relevant concentrations. Therefore, drug interactions with CYP2C8-substrates are unlikely. Vice versa, the inhibition of CYP2C8 by co-administered drugs such as montelukast might lead to decreased systemic exposure of M2 which, however, is without any consequences for the safety and efficacy of licofelone.

References

Alvaro-Gracia JM (2004) Licofelone - clinical update on a novel LOX/COX inhibitor for the treatment of osteoarthritis. *Rheumatology* **43** (Suppl. 1): i21-i25.

Bailey MJ, Dickinson RG (2003) Acyl glucuronide reactivity in perspective: biological consequences. *Chem Biol Interact* **145**:117-37.

Bakke OM, Manocchia M, de Abajo F, Kaitin KI and Lasagna L (1995) Drug safety discontinuations in the United Kingdom, the United States, and Spain from 1974 to 1993: a regulatory perspective. *Clin Pharmacol Ther* **58**:108-117.

Bias P, Buchner A, Klesser B and Laufer S. (2004) The gastrointestinal tolerability of the LOX/COX inhibitor, licofelone, is similar to placebo and superior to naproxen therapy in healthy volunteers: results from a randomized, controlled trial. *Am J Gastroenterol* **99**:611-618.

Bradford, M. M. (1976) A rapid and sensitive method for the quantitation of microgram quantities of protein utilizing the principle of protein-dye binding. *Anal Biochem* **72**:248-254.

Clària J. and López-Parra M. (2005) New Perspectives in the Modulation of the Eicosanoid Cascade in Inflammation. *Lett Drug Des Discov* **2**: 391-402.

Dai D, Zeldin DC, Blaisdell J Chanas B, Coulter SJ, Ghanayem BI and Goldstein JA (2001) Polymorphism in human CYP2C8 decrease metabolism of the anticancer drug paclitaxel and arachidonic acid. *Pharmacogenetics* **11**:597-607.

Delaforge M, Pruvost A, Perrin L and André F (2005) Cytochrome P450-mediated oxidation of glucuronide derivatives: Example of estradiol-17β-glucuronide oxidation to 2-hydroxy-estradiol-17β-glucuronide by CP 2C8. *Drug Metab Dispos* **33**:466-473.

Fisher MB, Campanale K, Ackermann BL, Vandenbranden M and Wrighton SA (2000) In vitro glucuronidation using human liver microsomes and the pore-forming peptide alamethicin. *Drug Metab Dispos* **28**:560-566.

Grillo MP, Knutson CG, Sanders PE, Waldon DJ, Hua F, Ware JA (2003) Studies on the chemical reactivity of diclofenac acyl glucuronide with glutathione: identification of diclofenac-S-acyl-glutathione in rat bile. *Drug Metab Dispos* **31**:1327-1336.

Grosser T, Fries S and FitzGerald GA (2006) Biological basis for the cardiovascular consequences of COX-2 inhibition: therapeutic challenges and opportunities. *J Clin Invest* **116**: 4-15.

Hashizume T, Imaoka S, Mise M, Terauchi Y, Fujii T, Miyazaki H, Kamataki T and Funae Y (2002) Involvement of CYP2J2 and CYP4F12 in the metabolism of ebastine in human intestinal microsomes. *J Pharmacol Exp Ther* **300**:298-304.

Kirschning, M, Ries S, Domann W, Martin Albrecht W, Arnold P and Laufer S (1997) Synthesis and biological identification of the acylglucuronide of the anti-inflammatory drug ML 3000. *Bioorg Med Chem Lett* **7**:903-906.

Kuehl GE, Lampe JW, Potter JD and Bigler J (2005) Glucuronidation of nonsteroidal anti-inflammatory drugs: Identifying the enzymes responsible in human liver microsomes. *Drug Metab Dispos* **33**:1027-1035.

Kulkarni SK and Singh VP (2007) Licofelone - a novel analgesic and anti-inflammatory agent. *Curr Top Med Chem* **7**:251-263.

Kumar S, Samuel K, Subramanian R, Braun MP, Stearns RA, Lee-Chiu S-H, Evans DC and Baillie TA (2002) Extrapolation of diclofenac clearance from in vitro microsomal metabolism data: role of acyl glucuronidation and sequential oxidative metabolism of the acyl glucuronide. *J Pharmacol Exp Ther* **303**:969-978.

Laufer SA, Augustin J, Dannhardt G and Kiefer W (1994) (6,7-Diaryldihydropyrrolizin-5-yl) acetic acids, a novel class of potential dual inhibitors of both cyclooxygenase and 5-lipoxygenase. *J Med Chem* **37**:1894-1897.

Matsumoto S, Hirama T, Matsubara T, Nagata K and Yamazoe Y (2002) Involvement of CYP2J2 on the intestinal first-pass metabolism of antihistamine drug, astemizole. *Drug Metab Dispos* **30**:1240-1245.

Moreau M, Daminet S, Martel-Pelletier J, Fernandes J, Pelletier JP (2005) Superiority of the gastroduoenal safety profile of licofelone over rofecoxib, a COX-2 selective inhibitor, in dogs. *J Vet Pharmacol Ther* **28**:81-86.

Moreau M, Lussier B, Doucet M, Vincent G, Martel-Pelletier J, Pelletier JP (2007) Efficacy of licofelone in dogs with clinical osteoarthritis. *Vet Rec* **160**:584-588.

Ogilvie BW, Zhang D, Li W, Rodrigues D, Gipson AE, Holsapple J, Toren P and Parkinson A (2006) Glucuronidation converts gemfibrotil to a potent, metabolism-dependent inhibitor of CYP2C8: Implications for drug-drug interactions. *Drug Metab Dispos* **34**:191-197.

Pearce RE, McIntyre CJ, Madan A, Sanzgiri U, Draper AJ, Bullock PL, Cook DC, Burton LA Latham J, Nevins C and Parkinson A (1996) Effects of freezing, thawing and storing human liver microsomes on cytochrome P450 activity. *Arch Biochem Biophys* **331**:145-169.

Sakaguchi K, Green M, Stock N, Reger TS, Zunic J and King Ch (2004) Glucuronidation of carboxylic acid containing compounds by UDP-glucuronosyltransferase isoforms. *Arch Biochem Biophys* **424**:219-225.

Shitara Y, Hirano M, Sato H and Sugiyama Y (2004) Gemfibrozil and its glucuronide inhibit the organic anion transporting polypeptide 2 (OATP2/OATP1B1:SLC21A6)-mediated hepatic uptake and CYP2C8-mediated metabolism of cerivastatin: Analysis of the mechanism of the clinically relevant drug-drug interaction between cerivastatin and gemfibrozil. *J Pharmacol Exp Ther* **311**: 228-236.

Skelly MM and Hawkey CJ (2003) COX-LOX Inhibition: Current evidence for an emerging new therapy. *Int J Clin Pract* **57**: 301-304.

Spahn-Langguth H, Dahms M and Hermening A (1996) Acyl glucuronides: covalent binding and its potential relevance. *Adv Exp Med Biol* **387**:313-328.

Stachulski AV (2007) The chemistry and biological activity of acyl glucuronides. *Curr Opin Drug Dis Dev* **10**:58-66.

Totah RA and Rettie AE (2005) Cytochrome P450 2C8: substrates, inhibitors, pharmacogenetics, and clinical relevance. *Clin Pharmacol Ther* **77**:341-352.

Tries S, Neupert W and Laufer S. (2002) The mechanism of action of the new anti-inflammatory compound ML3000: inhibition of 5-LOX and COX-1/2. *Inflamm Res* **51**:135-143.

Walsky RL, Obach RS, Gaman EA, Gleeson JPR and Proctor WR (2005a). Selective inhibition of human cytochrome P4502C8 by montelukast. *Drug Metab Dispos* **33**:413-418.

Walsky RL, Gaman EA and Obach RS (2005b). Examination of 209 drugs for inhibition of Cytochrome P450 2C8. *J Clin Pharmacol* **45**:68-78.

Wilson ZE, Rostami-Hodjegan A, Burn JL, Tooley A, Boyle J, Ellis SW and Tucker GT (2003) Inter-individual variability in levels of human microsomal protein and hepatocellularity per gram of liver. *Br J Clin Pharmacol* **56**:433-440.

Zamek-Gliszczynski MJ, Hoffmaster KA, Nezasa K, Tallman MN and Brouwer KLR (2006) Integration of hepatic drug transporters and phase II metabolizing enzymes: Mechanisms of hepatic excretion of sulfate, glucuronide, and glutathione metabolites. *Eur J Pharm Sci* **27**:447–486.

Footnotes

* present address: Department of Traumatology, TU Munich, Ismaninger Str. 22, 81675 Munich (Germany).

Acknowledgement

The hepatocyte work was partially supported by the Federal Ministry of Education and Research (BMBF 0313079B).

Request for reprints to: Dr. Wolfgang Albrecht, c-a-i-r biosciences GmbH, Paul-Ehrlich-Str. 15, D-72076 Tübingen (Germany), e-mail: w.albrecht@cair-biosciences.de

Legends for Figures

Figure 1: Chemical structure of licofelone and its proposed biotransformation pathway.

Figure 2: Biotransformation of licofelone in phase I assays with CYP-isoforms (n = 2, rates given as means). Metabolite concentrations were determined by LC-MS/MS and expressed as percent relative to the initial substrate concentration of 100 µM.

Figure 3: Biotransformation of licofelone in dual activity assay with HLM (n = 3, rates given as mean + s.d.). Bars illustrate the percentage biotransformation related to the initial substrate concentration and the numbers above the bars correspond to absolute concentrations.

top: hydroxy metabolites M2 and M4,

bottom: glucuronide conjugates M1 and M3

Figure 4: Effect of pre-incubation of M1 with microsomes on its biotransformation into M3. 10 µM and 30 µM M1 were added to HLM or CYP 2C8. Immediately or after 15 min pre-incubation, hydroxylation activity was initiated by addition of NADPH. M3 concentrations were determined after 30 min.

Figure 5: Effect of montelukast, licofelone and M1 on the rate of paclitaxel-6α-hydroxylation (n = 3, rates given as mean + s.d., Montelukast was only tested at concentrations of 1, 10, and 30 µM)

top: CYP2C8

bottom: HLM

DMD Fast Forward. Published on February 11, 2008 as DOI: 10.1124/dmd.108.020347
This article has not been copyedited and formatted. The final version may differ from this version.

Tables

Table 1: Metabolite concentrations after incubation of licofelone and diclofenac with liver microsomes from humans (HLM) and rats (RLM). In phase I assays, NADPH was added as co-substrate, in phase II assays, microsomes were pre-incubated with alamethicin and UDP-glucuronic acid was used as co-substrate. Concentrations are expressed as percent relative to the initial substrate concentration of 100 µM.

	Licofelone			**Diclofenac**	
	M1	M2	M4	DF-Gluc.	4'-OH-DF
Phase I-assay					
HLM	N/D*	0.06 %	1.8 %	N/D	> 90%
RLM	N/D	1.1 %	1.8 %	not performed	
Phase II-assays					
HLM	70 %	N/D	N/D	90%	N/D
RLM	95 %	N/D	N/D	80%	N/D

*: N/D = M1 not detected;

DMD Fast Forward. Published on February 11, 2008 as DOI: 10.1124/dmd.108.020347
This article has not been copyedited and formatted. The final version may differ from this version.

Table 2: Glucuronidation activity of tested UGT isoforms after incubation of 100 µM licofelone for 30 min. Relative M1 concentrations were determined by LC-MS/MS using ML3000 formic acid as ISTD and expressed as peak area ratios (M1/ISTD).

UGT Isoform	concentration of M1 [p.a.r.]
1A1	N/D*
1A3	12.493
1A6	N/D
1A7	7.581
1A9	13.334
1A10	N/D
2B7	44.847
2B15	0.108

*: N/D = M1 not detected;

DMD Fast Forward. Published on February 11, 2008 as DOI: 10.1124/dmd.108.020347
This article has not been copyedited and formatted. The final version may differ from this version.

Table 3: Concentrations of metabolites in cultures of human hepatocytes after incubation of 30 µM and 100 µM licofelone for 4 h and 24 h. Concentration data were converted into biotransformation rates (% of initial licofelone concentration, mean ± s.d., n=3).

Metabolite	Biotransformation [%]			
	time = 4 h		time = 24 h	
	30 µM*[1]	100 µM	30 µM	100 µM
M1	20.3 ± 13.9	7.28 ± 3.80	46.4 ± 8.5	24.3 ± 8.9
M2	0.11 ± 0.01	0.04 ± 0.01	0.91 ± 0.45	0.10 ± 0.06
M3	2.4 ± 2.2	0.22 ± 0.21	3.58 ± 2.10	0.75 ± 0.56
M4	0.08 ± 0.02	0.03 ± 0.01	0.17 ± 0.06	0.08 ± 0.03
M5	<*[2]	<	<	<

*[1]: licofelone substrate concentration;

*[2]: < = concentration below the limit of quantification;

DMD Fast Forward. Published on February 11, 2008 as DOI: 10.1124/dmd.108.020347
This article has not been copyedited and formatted. The final version may differ from this version.

Table 4: Concentrations of metabolites in phase I (cofactor: NADPH) and dual activity assays (cofactors: NADPH and UDPGA) after incubation of 10 µM licofelone for 30 min. Concentration data were converted into biotransformation rates (% of initial licofelone concentration; mean ± s.d., n=3).

		Biotransformation [%]					
Metabolite	Cofactors	man	monkey	dog	rabbit	rat	mouse
M1	NADPH	N/D*[1]	N/D	N/D	N/D	N/D	N/D
	NADPH + UDPGA	7.33 ± 1.14	28.3 ± 3.4	40.2 ± 3.6	25.9 ± 1.6	53.9 ± 6.2	21.9 ± 0.7
M2	NADPH	<*[2]	2.89 ± 0.16	N/D	8.00 ± 0.46	1.11 ± 0.09	<
	NADPH + UDPGA	1.02 ± 0.18	0.59 ± 0.11	N/D	4.01 ± 0.33	0.24 ± 0.04	<
M3	NADPH	N/D	N/D	N/D	N/D	N/D	N/D
	NADPH + UDPGA	26.8 ± 2.1	4.44 ± 0.51	N/D	3.48 ± 0.17	N/D	N/D
M4	NADPH	2.05 ± 0.16	0.69 ± 0.17	2.23 ± 0.14	0.18 ± 0.03	2.24 ± 0.12	0.57 ± 0.03
	NADPH + UDPGA	0.47 ± 0.04	0.14 ± 0.02	0.15 ± 0.03	<	0.48 ± 0.06	0.12 ± 0.02
M5	NADPH	N/D	N/D	N/D	N/D	N/D	N/D
	NADPH + UDPGA	N/D	N/D	N/D	N/D	N/D	N/D
total	NADPH	2.05 ± 0.16	3.58 ± 0.18	2.23 ± 0.14	8.18 ± 0.43	3.35 ± 0.18	0.57 ± 0.03
	NADPH + UDPGA	35.6 ± 1.7	33.5 ± 3.9	40.4 ± 3.6	33.4 ± 2.0	54.6 ± 6.3	22.0 ± 0.7

*[1] N/D = not detected,

*[2] < = concentration below limit of quantification;

DMD Fast Forward. Published on February 11, 2008 as DOI: 10.1124/dmd.108.020347
This article has not been copyedited and formatted. The final version may differ from this version.

Table 5: Biotransformation of 3 µM M1 into M3 in microsomal preparations (n=1).

Microsomal preparation	Biotransformation [%]
HLM	> 90%
CLM	35%
RLM	<
MLM	<
CYP2C8	50%
other CYPs*[1]	N/D*[2]

*[1]tested: CYP 1A2, 2A6, 2B6, 2C9, 2C19, 2D6, 2E1, 3A4, 2J2, 4F12;

*[2] N/D = not detected;

DMD Fast Forward. Published on February 11, 2008 as DOI: 10.1124/dmd.108.020347
This article has not been copyedited and formatted. The final version may differ from this version.

Table 6: Effect of montelukast on the formation of metabolites of licofelone in dual activity assays (mean ± s.d., n=3). Solvent or 1, 10 and 30 µM montelukast were added to microsomes immediately prior to the addition of 30 µM licofelone.

	Biotransformation [%]			
Montelukast [µM]	M1	M2	M3	M4
0	17.4 ± 1.9	0.45 ± 0.07	25.8 ± 4.1	0.44 ± 0.03
1	19.1 ± 1.3	0.37 ± 0.05	22.5 ± 1.5	0.38 ± 0.06
10	36.0 ± 1.0	0.11 ± 0.01	8.11 ± 1.12	0.34 ± 0.02
30	41.2 ± 1.7	<*	2.41 ± 0.17	0.23 ± 0.03

* < = concentration below limit of quantification

DMD Fast Forward. Published on February 11, 2008 as DOI: 10.1124/dmd.108.020347
This article has not been copyedited and formatted. The final version may differ from this version.

Table 7: Biotransformation of 30 µM licofelone in dual activity assays with microsomes from extrahepatic tissues.

microsomes	Biotransformation [%]	
	human	monkey
Intestine	21.0	38.0
Kidney	33.0	N/T
lung	0.2	N/T

N/T = not tested

Figure 1:

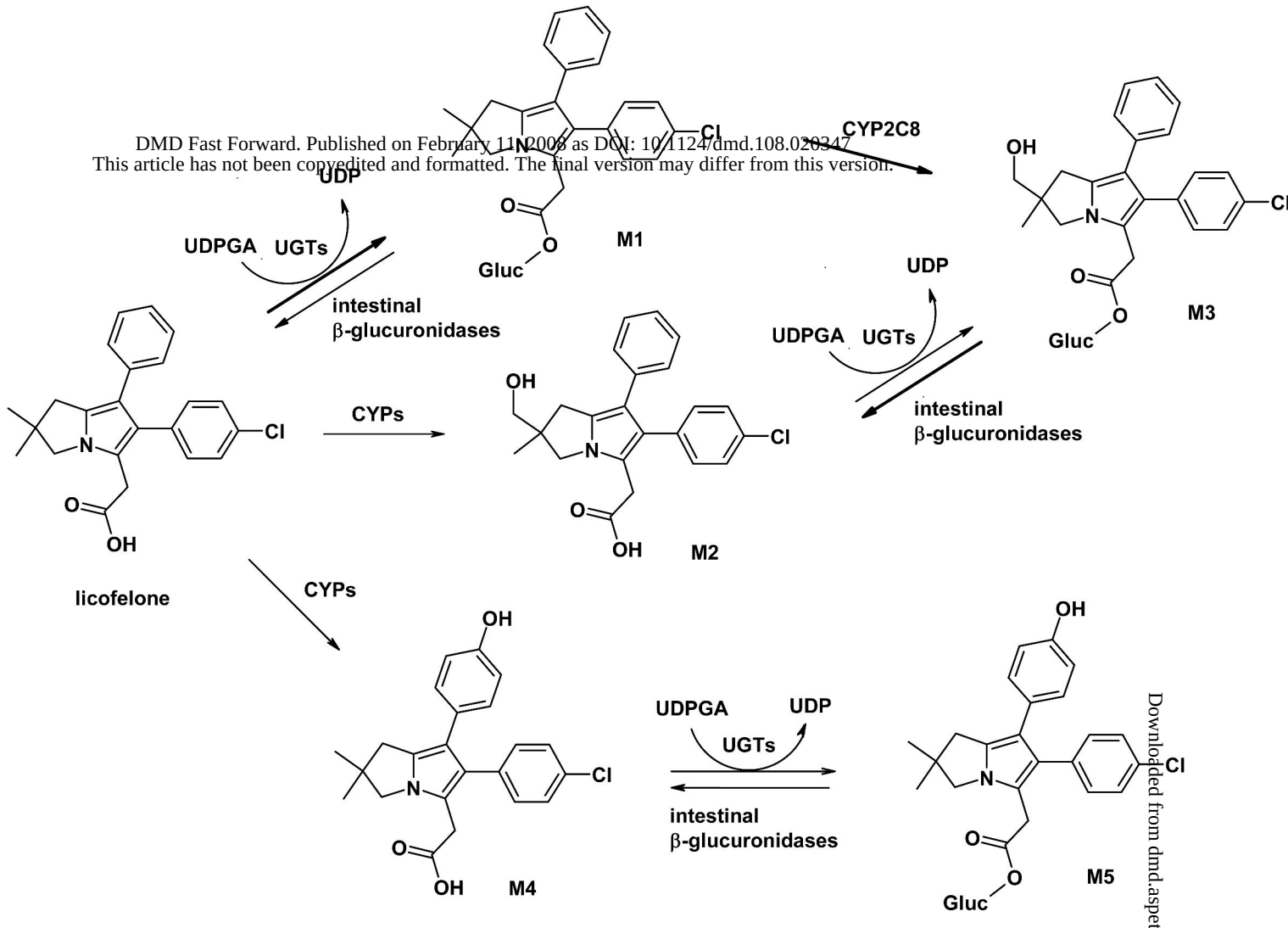

Figure 2:

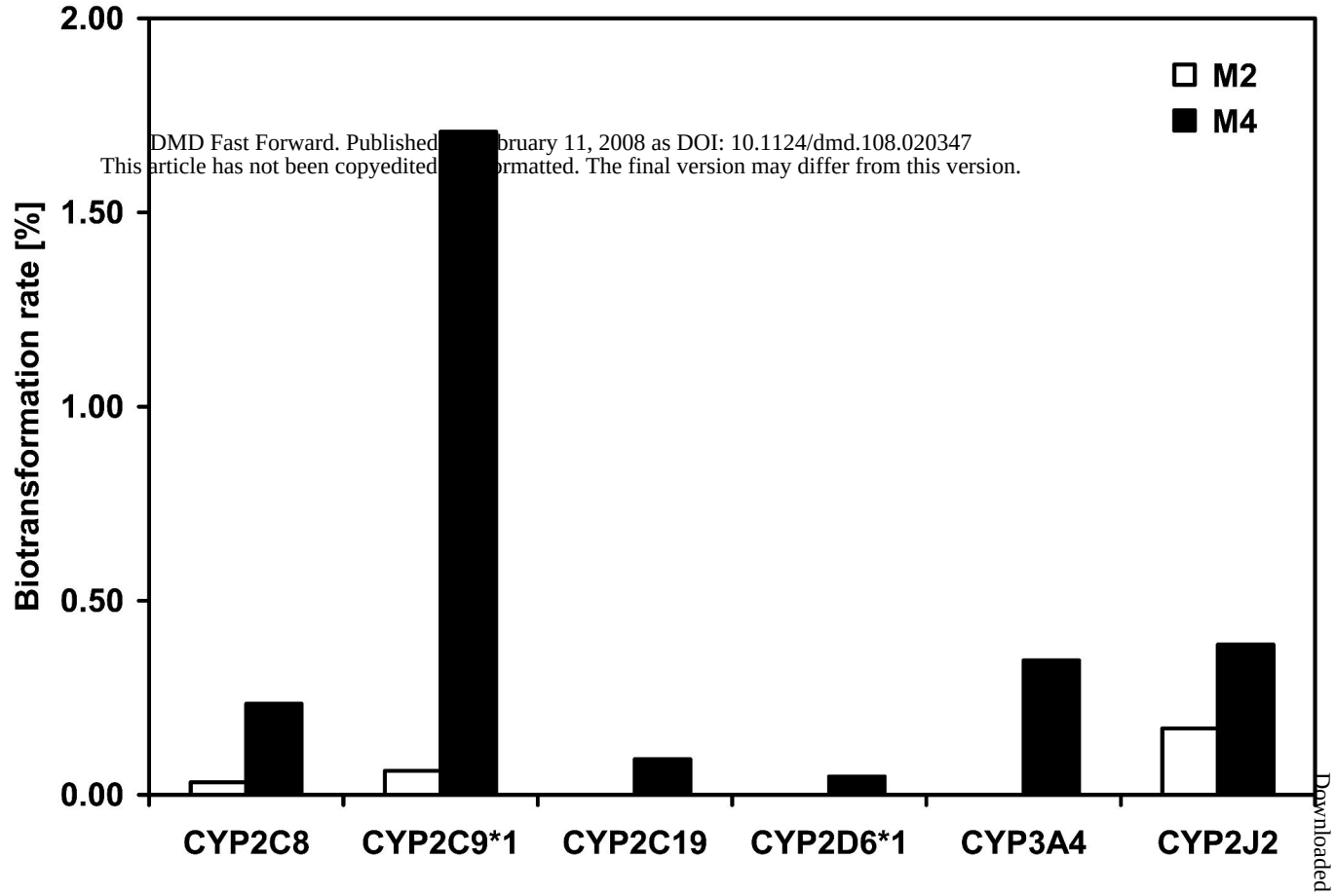

Figure 3:

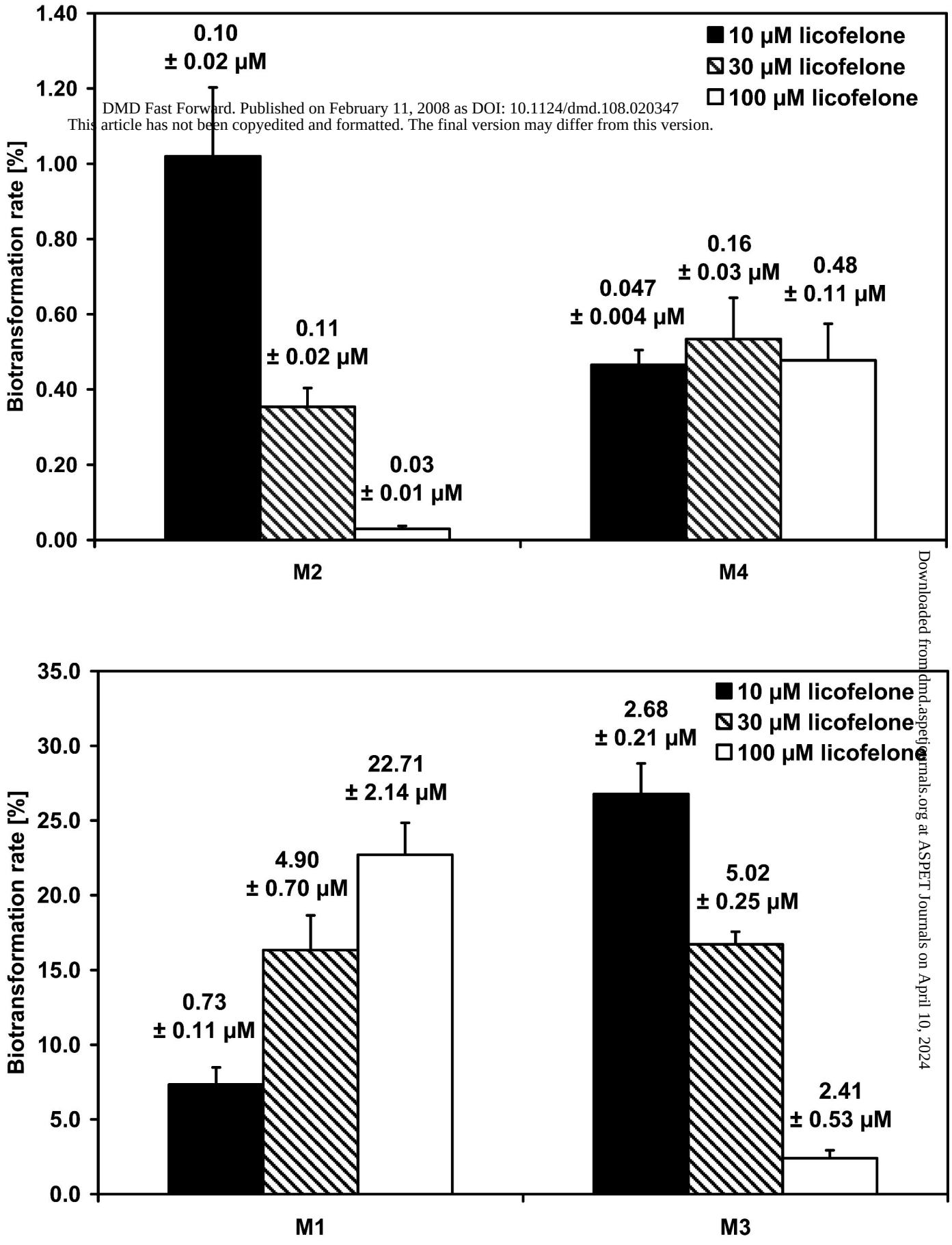

DMD Fast Forward. Published on February 11, 2008 as DOI: 10.1124/dmd.108.020347

Figure 4:

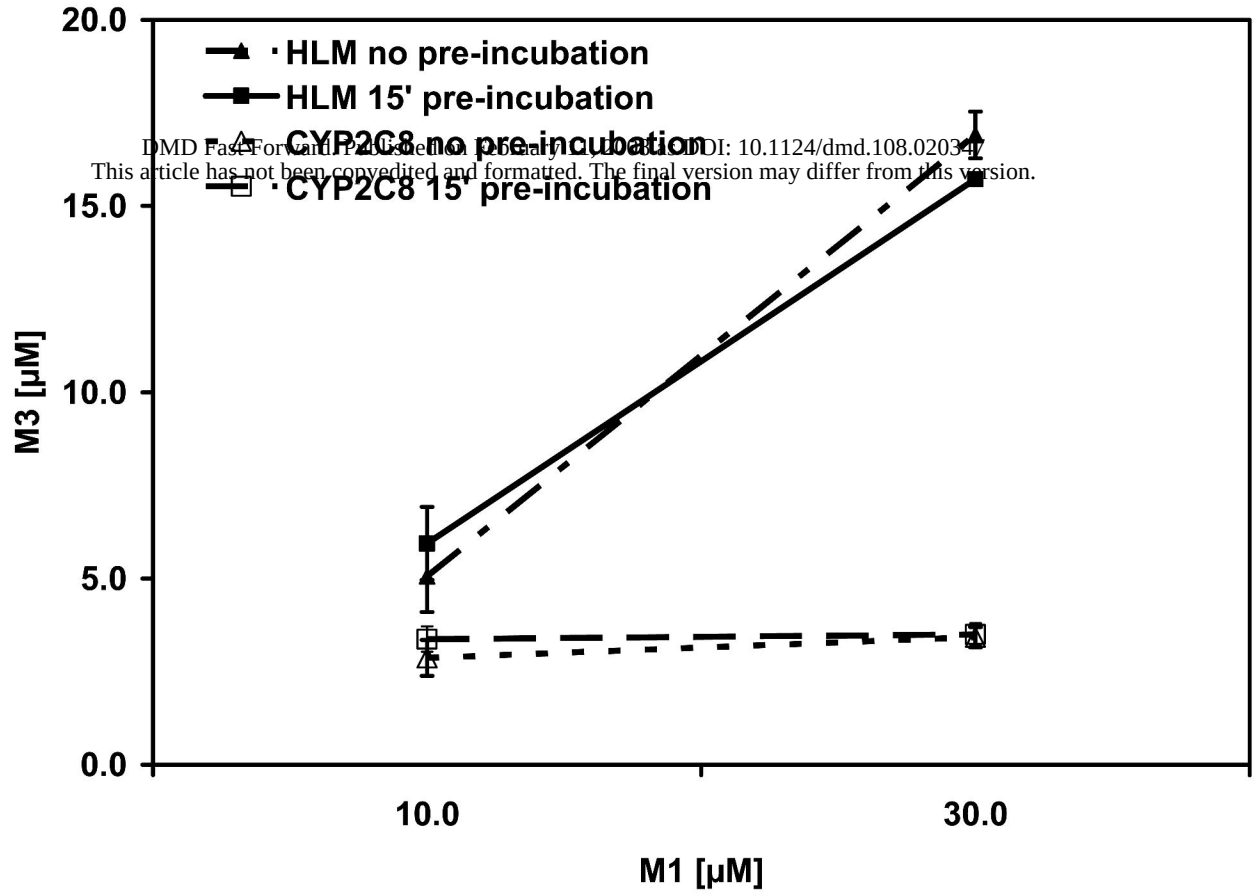

Figure 5: